

LARGE-SCALE COSMIC SHEAR MEASUREMENTS

NICK KAISER, GILLIAN WILSON AND GERARD A. LUPPINO

Institute for Astronomy, U. Hawaii

2680 Woodlawn Drive, Honolulu, Hawaii 96822

kaiser@hawaii.edu, <http://www.ifa.hawaii.edu/~kaiser>*Draft version March 23, 2000*

ABSTRACT

We present estimates of the gravitational lensing shear variance obtained from images taken at the CFHT using the UH8K CCD mosaic camera. Six fields were observed for a total of 1 hour each in V and I, resulting in catalogs containing $\sim 20,000$ galaxies per field, with properly calibrated and optimally weighted shear estimates. These were averaged in cells of sizes ranging from $1'.875$ to $30'$ to obtain estimates of the cosmic shear variance $\langle \bar{\gamma}^2 \rangle$, with uncertainty estimated from the scatter among the estimates for the 6 fields. Our most reliable estimator for cosmic shear is provided by the cross-correlation of the shear measured in the two passbands. At scales $\lesssim 10'$ the results are in good agreement with those of Van Waerbeke et al. (2000), Bacon et al. (2000) and Wittman et al. (2000) and with currently fashionable cosmological models. At larger scales the shear variance falls below the theoretical predictions, and on the largest scales we find a null detection of shear variance averaged in $30'$ cells of $\langle \bar{\gamma}^2 \rangle = (0.28 \pm 1.84) \times 10^{-5}$.

Subject headings: Cosmology: observations — dark matter — gravitational lensing — large-scale structure of Universe — galaxies: photometry

1. INTRODUCTION

Weak lensing provides a potentially powerful probe of mass fluctuations in the Universe (Gunn 1967; Mellier 1999, and references therein). Three independent groups have recently presented estimates of the shear variance from deep ‘blank-field’ CCD imaging surveys. Van Waerbeke et al. (2000, hereafter vWME+) measured the shear variance in circular cells of radii ranging from $0'.7$ to $3'.5$; Bacon, Refregier, & Ellis (2000, hereafter BRE) measured the shear variance in square cells of side $8'.0$ and Wittman et al. (2000, hereafter WTK+) have provided estimates of the shear-shear correlation function at separations $3'.25$, $8'.5$ and $22'.0$. Here we present shear variance measurements from $\simeq 1.5$ square degrees of deep photometry obtained as part of our ongoing weak lensing survey. We find results which are broadly in good agreement with the recently published estimates.

2. THE DATA

The data were taken at the 3.6m CFHT telescope using the 8192×8192 pixel UH8K camera at prime focus. The camera delivers a field size of $0^\circ.5$ with $0''.207$ pixels. Our survey strategy has been to target blank fields in six widely separated areas for ease of scheduling, and in each area we plan to make 6 or so pointings scattered over a region of extent $\sim 3^\circ$. In January 1999 the UH8K was replaced by the CFH12K camera. By that time we had completed 1 hour integrations in both V and I for two pointings in each of three areas. The field names, centers and also the estimated seeing are given in table 1. One of the 8 devices in the mosaic (lying in the NW corner of our images) has very poor charge transfer efficiency and the data from this device were discarded. After further masking of regions around bright stars the total useful solid angle per field is $\simeq 0.16$ square degrees.

3. DATA REDUCTION

The data were reduced much as for our MS0302 supercluster observations (Kaiser et al. 1999). After flat fielding, an ob-

ject finder was applied to each image, and a set of bright but non-saturated stars extracted for registration purposes. The positions of these stars, along with celestial coordinates from the USNOA (Monet 1998) catalog, were used to find a mapping from image pixel coordinates to orthographic sky coordinates.

Images of the stars were analyzed to generate a model for the point spread function (PSF) $g(\mathbf{x}; \mathbf{r})$, this being the 2-dimensional profile of a star with centroid at \mathbf{r} measured in coordinates \mathbf{x} being measured relative to the centroid. The model is a sum of 2-D image valued modes $g_i(\mathbf{x})$: $g(\mathbf{x}; \mathbf{r}) = \sum_i c_i(\mathbf{r}) g_i(\mathbf{x})$ with coefficients $c_i(\mathbf{r})$ which are low order polynomials in star position. We found a 1st order model to be adequate to describe the variation of the PSF with position on the chip (though see below).

The astrometric solutions, the PSF models, and also standard star observations were first used to create a set of photometrically calibrated ‘homogenized’ images which were degraded to have a common identical PSF. These images were compared in order to identify cosmic rays and other transient events. Next, for each raw image we generated a re-circularized image by convolving with a 90-degree rotated version of the PSF model. These, as well as the raw images, were then warped to sky coordinates, with previously identified cosmic rays being removed, and the stacks of images combined to provide a quilt of overlapping images. This procedure results in three images: a median of the raw images (in which the PSF is generally non-circular), a median of the re-circularized images, and also a sky-noise image. The final summed images were sampled with $0''.15$ pixel size.

The final object catalogs were obtained by applying `hfind-peaks` to the median averaged raw images, this program having been modified in order to allow properly for the non-trivial noise correlations in the final images. After applying aperture photometry analysis, shapes of the objects were measured as described by Kaiser (2000). The essential result of this is a polarization vector $q_\alpha = M_{\alpha lm} \int d^2x w(x) x_l x_m f(\mathbf{x})$ formed as a

TABLE 1
FIELD CENTERS AND SEEING

area	pointing	RA (J2000)	DEC (J2000)	l	b	FWHM(I)	FWHM(V)
1650	1	16:51:49.0	34:55:2.0	57.37	38.67	0".82	0".85
	3	16:56:0.0	35:45:0.0	58.58	37.95	0".85	0".72
Groth	1	14:16:46.0	52:30:12.0	96.60	60.04	0".80	0".93
	3	14:9:0.0	51:30:0.0	97.19	61.57	0".70	0".85
Lockman	1	10:52:43.0	57:28:48.0	149.28	53.15	0".83	0".85
	2	10:56:43.0	58:28:48.0	147.47	52.83	0".84	0".86

combination of weighted second moments of the re-circularized image, and a polarizability tensor which describes the response of the polarization to gravitational shear. The weight function $w(x)$ was taken to be a Gaussian ball of 2 pixels in scale length. For convenience, the quantities actually generated were the normalized polarization $\hat{q}_\alpha = q_\alpha / \sqrt{q_\beta q_\beta}$ and a polarizability Q defined such that for galaxies with this shape and size, the expectation value of \hat{q}_α is $\langle \hat{q}_\alpha \rangle = Q\gamma_\alpha$. The q_α values were corrected for artificial shear introduced in the image warping by slight errors in our astrometric solution.

Finally a selection on significance of $4 \leq \nu \leq 100$ was applied to select a ‘faint galaxy’ catalog. The corresponding magnitude limits are somewhat fuzzy since significance depends on both size and magnitude. The counts (number per magnitude interval) turn over at about $m_I \simeq 24$ and $m_V \simeq 25$. Numbers of objects in the final catalogs are shown in table 2. The density of objects on the sky is very similar to that in the images obtained by vWME+, WTK+, and slightly higher than the density of objects in the BRE sample, so our shear variance estimates should be more or less directly comparable.

Given a single galaxy, a fair (but very noisy) estimate of the shear is $\gamma_\alpha = \hat{q}_\alpha / Q$. However, since the normalized polarization response Q varies with shape and size of the object (small objects having very little response for example), to measure the mean shear in a region containing N galaxies one should weight the individual estimates by Q^2 so the optimal mean shear estimate is $\bar{\gamma}_\alpha = \sum Q\hat{q}_\alpha / \sum Q^2$. This assumes that one has little prior knowledge of the of galaxy redshifts. If the averaging region contains a large number of galaxies, as is the case for the cells considered here, one can replace $\sum Q^2$ by $N\langle Q^2 \rangle$ where the $\langle Q^2 \rangle$ is an average over all of the galaxies in the catalog. The optimal mean shear is then the average of weighted shear values for the individual galaxies: $\gamma_G = \omega_G \hat{q}_G / Q_G$, with normalized weight $\omega_G \equiv Q_G^2 / \langle Q^2 \rangle$. The quantity $\langle Q^2 \rangle$ is a useful measure of the image quality. It is equal to the inverse shear variance per galaxy, so, for instance, the statistical uncertainty in the mean shear $\bar{\gamma}$ measured from a sample of N galaxies is $\sigma_{\bar{\gamma}}^2 = 1 / (N\langle Q^2 \rangle)$. The values of $\langle Q^2 \rangle$ are also given in table 2.

Preliminary results of this analysis (Wilson et al. 1999) in the form of estimates of the net shear for each of the six fields and for catalogs generated from the I and V images separately gave shear values typically of about 1%, but with a few larger values. These, however, showed little correlation between the two passbands, suggesting that the results were contaminated by some systematic error. Examination of the re-circularized images of the stars in the fields with seemingly spurious shear values revealed at least a major part of the problem. The mean stellar polarization was found to vary systematically with magnitude. This is to be expected for very bright stars where the

pixels saturate and charge begins to bleed along the slow direction of the CCD. The effect found here had the same signature (a trend for q_1 to become negative for bright objects) but appeared at a low level and, unexpectedly, for stars much fainter than the saturation limit. The result was that in some cases our PSF model fitting procedure, which weighted stars according to brightness, did not correctly recircularize the faint stars as it should (since we require the PSF appropriate for faint galaxies). The effect seemed to be variable, and also tended to be associated with particular chips. As a simple fix, we fit the residual polarizations for the faintest stars ($I > 18, V > 21$) to a 4th order spatial polynomial and then used a smear polarizability analogous to that defined by Kaiser et al. (1995) to correct the galaxy q_α values. This reduced the spurious shear values considerably.

TABLE 2
GALAXY CATALOGS

field	N_I	$\langle Q^2 \rangle_I$	N_V	$\langle Q^2 \rangle_V$
1650 1	21569	1.527	15403	1.234
1650 3	18187	1.785	16518	1.147
Groth 1	27293	1.440	16391	1.543
Groth 3	19162	1.254	15876	1.775
Lockman 1	20726	1.855	20358	1.352
Lockman 2	20017	1.630	17779	1.417

4. COSMIC SHEAR VARIANCE

We have chosen to focus here on a single simple statistic: the variance of the shear averaged in cells of various sizes. This is the statistic used by vWME+ and BRE and is simply related to the shear covariance function presented by WTK+. The cell averaged shear variance is also simply computable from the spectrum of mass fluctuations (e.g., Kaiser 1992), so this provides a useful link between observation and theory. Now each weighted shear estimate γ_G consists of a random intrinsic component γ_{Gint} and a ‘cosmic’ component proportional to the integral of the tidal field along the line of sight. Modeling the cosmic shear as the sum over a set of statistically independent screens, we have

$$\gamma_G = \gamma_{Gint} + \omega_G \sum_S \gamma_S(\theta_G) \beta(z_G, z_S) \quad (1)$$

where $\gamma_S(\theta)$ is the shear field for the S th screen and for fictitious sources at infinite distance, and $\beta \equiv \max(0, 1 - D_{SG}/D_{OG})$ is the usual ratio of angular diameter distances.

This model allows one to compute the variance of the shear averaged over galaxies falling in a cell on the sky. We will also be interested in the co-variance of shear measured in different passbands. Consider the mean shear $\bar{\gamma}_P = (1/N_P) \sum \gamma_P$ for a specific cell and for galaxies found in two passbands $P = A, B$. Averaging over realizations of random intrinsic shear values,

and also averaging over an ensemble of realizations of cosmic shear screens, yields

$$\langle \bar{\gamma}_A \cdot \bar{\gamma}_B \rangle = \frac{N_{AB}}{N_A N_B} \langle \gamma_A \cdot \gamma_B \rangle + \sum_S \langle \omega_A \beta_{AS} \rangle \langle \omega_B \beta_{BS} \rangle \langle \bar{\gamma}_S^2 \rangle \quad (2)$$

where N_{AB} is the number of objects in the cell which were detected in both passbands. This formula is also valid when A and B are the same. The expectation value of the dot product of the cell averaged shear is therefore equal to a noise term plus a cosmic term which is a sum of the cell-averaged shear variances for the screens. Interestingly, the noise term involves the total shear variance $\langle \gamma_A \cdot \gamma_B \rangle$, containing both intrinsic and cosmic contributions, which is convenient since this is the quantity that one can actually measure. In obtaining (2) we assumed that the faint galaxies are randomly distributed on the sky, this being motivated by the fact that the angular correlation function is very small, with $w(\theta) \lesssim 10^{-2}$ on all relevant scales.

To implement this, for each field we averaged the shear in a grid of contiguous square cells of side L , and those cells in the lower quartile of occupation number were discarded. To obtain an estimate of the cosmic shear variance we then computed for each field

$$\langle \bar{\gamma}^2 \rangle_{AB} = \frac{1}{n_{\text{cells}}} \sum_{\text{cells}} [\bar{\gamma}_A \cdot \bar{\gamma}_B - N_{AB} \langle \gamma_A \cdot \gamma_B \rangle / (N_A N_B)]. \quad (3)$$

The shear covariance functions are $\langle \gamma_I \cdot \gamma_I \rangle = 1/\langle Q^2 \rangle_I$ and $\langle \gamma_V \cdot \gamma_V \rangle = 1/\langle Q^2 \rangle_V$ whereas $\langle \gamma_I \cdot \gamma_V \rangle$ was estimated by correlating the shears for objects which were detected in both the I and V catalogs. The shear variances estimated from the separate fields were then averaged together to obtain a final cosmic shear variance with uncertainty estimated from the scatter of the field estimates about the mean.

The diagonal components of $\langle \bar{\gamma}^2 \rangle_{AB}$ provide estimates for the shear variance for the respective passbands, with strength roughly proportional to the square of the mean distance to the galaxies (assuming a spectrum of mass fluctuations with index $n \simeq -1$), and the off-diagonal components should lie somewhere in between. The results are shown in figure 1 and in table 3 and deviate somewhat from this expectation: the I-V cross correlation lies systematically below both the I- and V-band shear variance estimates. These results are robust to changes in the order of the polynomial in the stellar polarization model, and they are not caused by a few discrepant cells.

The difference between the I and V band shear variance may be due to differences in the redshift distributions, some evidence for which was found by Luppino & Kaiser (1997) in their study of MS1054. However, we typically find about 60% of the galaxies are detected in both passbands, so this requires fairly high redshifts for the blue galaxies. For example, assume that the I-band sample has a redshift distribution like that measured by Cowie (personal communication) in the range $23 < I_{AB} < 24.0$, but that the V band sample contains an additional 40% population of higher redshift galaxies. If we place these at redshift 3, we find that the V-band shear variance is about a factor 2 higher than the I-band, much as seen in figure 1. However the I-V cross-correlation is then predicted to be about 30% higher than the I-band variance, which is not seen.

The simplest interpretation of these results is that the shear inferred from the I- and V-band data separately has been inflated by residual systematic errors of some kind. The level of these errors is on the order of 2 percent rms shear on scales of a few arc-minutes, falling to somewhat below the 1 percent level on $30'$ scales. If so, the most reliable estimate of the cosmic

shear variance is provided by the I-V cross-correlation since systematic errors which are uncorrelated between the passbands will cancel out. Of course there is no guarantee that the cross-correlation is not affected by some source of error which is common to both passbands, a specific example of which is artificial shear arising from intrinsic correlation of galaxy shapes in clusters etc. due to tidal effects.

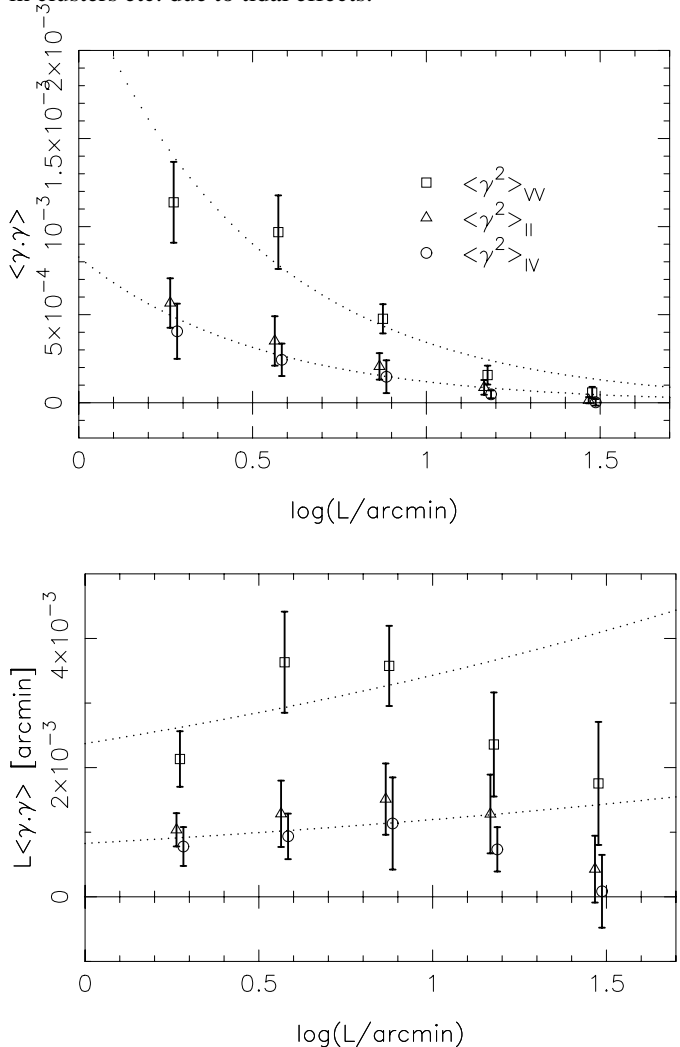


FIG. 1.— Estimates of the cosmic shear variance as a function of averaging scale L . Lower panel shows the same data multiplied by L to show more clearly the large angular scale results. The dotted lines are predictions for a currently fashionable cosmological model — cluster normalised; $\Omega_m = 0.3$; $\Omega_\Lambda = 0.7$; $\Gamma = 0.25$ — from Jain & Seljak (1997) for sources with an effective redshift (i.e. equivalent single screen redshift) of $z_{\text{eff}} = 1.0$ and $z_{\text{eff}} = 2.0$. The points have been displaced slightly laterally for clarity.

The I-V shear variance estimator is shown with an expanded vertical scale in figure 2. Also shown are the recently announced results. The BRE result is shown as presented in their paper and with total error estimate including cosmic variance. The vWME+ circular cell average shear are plotted against $L = \sqrt{\pi}\theta$. The vWME+ error bars are statistical only. WTK+ presented estimates of the ellipticity correlation function $C_1(\theta) = \langle \epsilon_1(0)\epsilon_1(\theta) \rangle$. We have converted their $C_1(\theta)$ to an equivalent shear variance using formulae from Kaiser (1992) with $\epsilon = 2\gamma$ and assuming a spectral index $n = -1$. The lower panel shows the variance multiplied by averaging box size L . For a $n = -1$ spectrum, corresponding to a mass auto-correlation function $\xi(r) \propto 1/r^2$, this quantity should independent of scale.

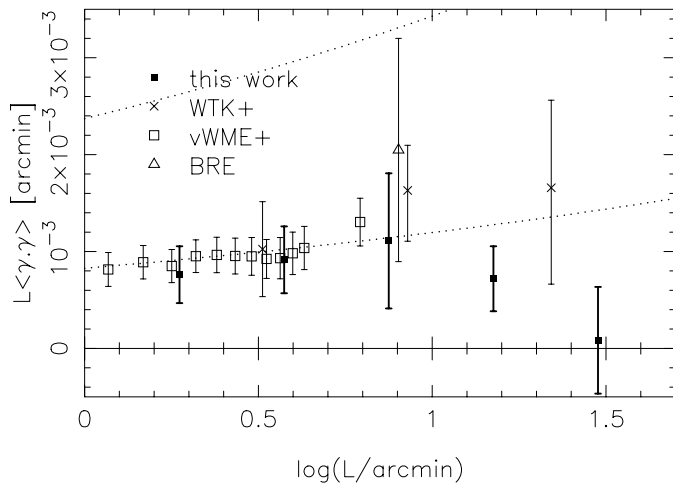
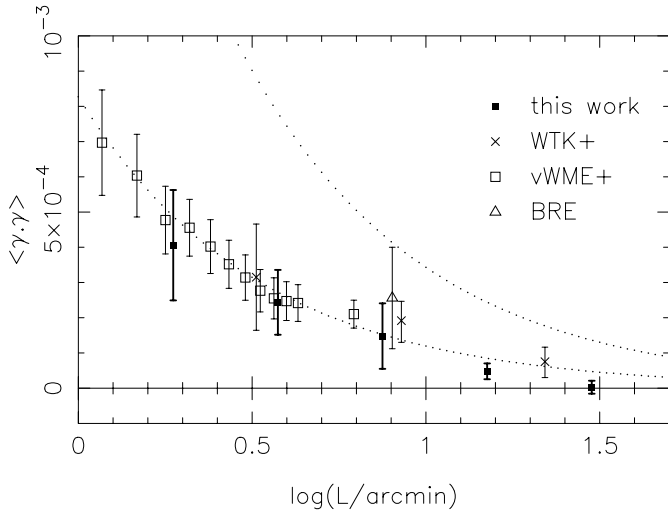


FIG. 2.— Our estimates of the cosmic shear variance from the I-V cross-correlator are shown as the heavy points. Also shown are results from vWME+, BRE, WTK+. The error bars on the vWME+ estimates are statistical only. All others are total error including cosmic variance. The lower panel again shows the same data multiplied by L to show more clearly the large angular scale results. The dotted lines are the Jain & Seljak (1997) predictions as in figure 1.

At small scales $\lesssim 10$ arcmin there seems to be remarkably good agreement between the independent estimates. Note that the measurements were made using three separate observing facilities. At $L = 3'.75$ we find $\langle \bar{\gamma}^2 \rangle \simeq 2.5 \simeq 10^{-4}$. This about a factor 4-5 lower than the prediction for a light-traces mass

$\Omega_m = 1$ cosmology, and an effective redshift for the background galaxies $z_{\text{eff}} = 1$ (Kaiser 1992; Jain & Seljak 1997).

At larger scales the shear variance we find falls below that of WTK+. Their largest scale estimates appear to conflict with our null result at about the 2-sigma level. Our large-angle results are also smaller than the $\Omega_m = 0.3$, $\Omega_\Lambda = 0.7$ theoretical model predictions.

TABLE 3
SHEAR VARIANCE

L/arcmin	$10^4 \times \langle \bar{\gamma}^2 \rangle_{\text{II}}$	$10^4 \times \langle \bar{\gamma}^2 \rangle_{\text{VV}}$	$10^4 \times \langle \bar{\gamma}^2 \rangle_{\text{IV}}$
30	0.15 ± 0.18	0.59 ± 0.32	0.03 ± 0.18
15	0.87 ± 0.42	1.57 ± 0.54	0.48 ± 0.22
7.5	2.06 ± 0.75	4.77 ± 0.83	1.48 ± 0.93
3.75	3.51 ± 1.40	9.69 ± 2.09	2.44 ± 0.92
1.875	5.66 ± 1.40	11.38 ± 2.29	4.06 ± 1.57

5. DISCUSSION

For an effective background galaxy redshift of $z_{\text{eff}} \simeq 1.0$ these measurements probe mass fluctuations in a shell peaked at $z \simeq 0.4$. At this redshift the $30'$ field size corresponds to a comoving distance of about $6h^{-1}\text{Mpc}$, so the cell variances presented here probe scales in the range $0.4 - 6h^{-1}\text{Mpc}$. On the smaller end of this scale we find very good agreement with recently announced estimates from other groups, and also with canonical cosmological theory predictions. It is hard to definitively rule out the possibility that the small angle measurements are inflated by systematic errors, but one can safely rule out theories such as light-traces mass high density models which predict shear variance a factor ~ 5 higher than our results.

On larger scales our measurements are extremely precise, yet we find only a null detection for our largest cells. These results show that on large scales the rms shear is at most a fraction of a percent. The apparent discrepancy between these results and the theoretical predictions is quite interesting, and suggests a steepening of the mass correlation function at scales $\sim 1 - 2h^{-1}\text{Mpc}$. More data are needed however to definitively confirm this.

6. ACKNOWLEDGEMENTS

The results here were extracted from data taken at the Canada France Hawaii Telescope. The analysis was supported by NSF grants AST95-00515, AST99-70805. GW gratefully acknowledges financial support from the estate of Beatrice Watson Parrent and from Mr. & Mrs. Frank W. Hustace, Jr. We thank Peter Schneider and Gary Bernstein for helpful comments.

REFERENCES

- Bacon, D., Refregier, A., & Ellis, R. 2000, MNRAS submitted, astro-ph/0003008, BRE
 Gunn, J. 1967, ApJ, 147, 61+
 Jain, B. & Seljak, U. 1997, ApJ, 484, 560+
 Kaiser, N. 1992, ApJ, 388, 272
 Kaiser, N. 2000, ApJ in press, astro-ph/99004003
 Kaiser, N., Squires, G., & Broadhurst, T. 1995, ApJ, 449, 460
 Kaiser, N., Wilson, G., Luppino, G., & Dahle, H. 1999, PASP in press, astro-ph/9907229
 Luppino, G. & Kaiser, N. 1997, ApJ, 475, 20
 Mellier, Y. 1999, ARA&A, In press
 Monet, D. 1998, <http://archive.eso.org/skycat/servers/usnoa>
 Van Waerbeke, L., Mellier, Y., Erben, T., Cuillandre, J.-C., Bernardau, F., Maoli, R., Bertin, E., McCracken, H., Le Fèvre, O., Fort, B., Dantel-Fort, M., Jain, B., & Schneider, P. 2000, A&A submitted, astro-ph/0002500, vWME+
 Wilson, G., Kaiser, N., & Luppino, G. 1999, in Boston Gravitational Lensing Conference, ed. T. Brainerd & C. Kochanek
 Wittman, D., Tyson, J., Kirkman, D., Dell'Antonio, I., & Bernstein, G. 2000, Nature in press, astro-ph/0003013, WTK+